Applied Catalysis B: Environmental 90 (2009) 628–632

Contents lists available at ScienceDirect

Applied Catalysis B: Environmental

journal homepage: www.elsevier.com/locate/apcatb

Reforming methanol to electricity in a high temperature PEM fuel cell

George Avgouropoulos [a,*], Joan Papavasiliou [a], Maria K. Daletou [a], Joannis K. Kallitsis [a,b], Theophilos Ioannides [a], Stylianos Neophytides [a,c,**]

[a] Foundation for Research and Technology-Hellas (FORTH), Institute of Chemical Engineering and High Temperature Chemical Processes (ICE-HT), Stadiou Str., Platani, P.O. Box 1414, GR-26504 Patras, Greece
[b] Department of Chemistry, University of Patras, GR-26504 Patras, Greece
[c] Advent Technologies SA, Patras Science Park, Stadiou str., Platani, GR-26504, Greece

ARTICLE INFO

Article history:
Received 11 February 2009
Received in revised form 8 April 2009
Accepted 25 April 2009
Available online 3 May 2009

Keywords:
High temperature PEM fuel cell
Internal reforming
Methanol
Hydrogen

ABSTRACT

In this paper we demonstrate for the first time a compact power unit, where a methanol reforming catalyst is incorporated into the anode of a PEMFC. The proposed internal reforming methanol fuel cell (IRMFC) mainly comprises: (i) a H_3PO_4-imbibed polymer electrolyte based on aromatic polyethers bearing pyridine units, able to operate at 200 °C and (ii) a 200 °C active and with zero CO emissions Cu–Mn–O methanol reforming catalyst supported on copper foam. Methanol is being reformed inside the anode compartment of the fuel cell at 200 °C producing H_2, which is readily oxidized at the anode to produce electricity. The IRMFC showed promising electrochemical behavior and no signs of performance degradation for more than 72 h.

1. Introduction

Among the various types of fuel cells, polymer electrolyte membrane fuel cells (PEMFCs) seem to be the most technically advanced energy conversion system for stationary and mobile applications and have the highest potential for market penetration [1–4]. However, the use of pure H_2, especially for mobile applications, is hindered by problems of storage, safety and refueling. On the other hand, the lack of a worldwide infrastructure for transport and distribution of pure H_2, in addition with the presence of well-established and developed fossil fuel-based network, favors the near term solution of on-site (stationary) or on-board (mobile) hydrogen production from reforming of various hydrocarbons or alcohols [1,2,5].

Methanol has the benefits of having energy densities fivefold to sevenfold greater than that of standard compressed H_2 [1–5]. It is sulfur-free, easily handled, stored and transported. Moreover, methanol can be produced from renewable sources (e.g. biomass). Its most interesting application in fuel cell technology is its direct electrochemical oxidation on PtRu anode of direct methanol fuel cell, though with low prohibitive electrical efficiency for large scale applications [6,7]. Recently Haile et al. [8–10] demonstrated a direct methanol solid acid (CsH_2PO_4) fuel cell operating at 243 °C. However, its peak power output was less than half compared to operation with H_2-rich reformate gas. By integrating a $Cu/ZnO/Al_2O_3$ catalyst in the anode chamber they achieved a power density of 225 mW cm^{-2}, thus approaching the power densities achieved in the same system with reformate gas. Samms and Savinell [11] studied the same concept by using a high temperature H_3PO_4/polybenzimidazole (PBI) fuel cell at 220 °C. However, inherent problems related to the cell configuration and the properties of the employed materials at these elevated temperatures, caused severe deactivation of the $Cu/ZnO/Al_2O_3$ catalyst mainly due to the corrosion of Cu by H_3PO_4.

In this work, we present a novel internal reforming methanol high temperature PEM fuel cell. The main concept is the incorporation of a methanol reforming catalyst into the anodic compartment of the fuel cell, so that methanol reforming takes place inside the fuel cell. The proposed configuration is presently under test for an experimental proof of concept.

2. Experimental

TPS® was synthesized according to published procedure [12,13]. It is an aromatic poly(aryl ether sulfone) copolymer containing 2,5-biphenyl-pyridine and tetramethyl biphenyl moieties, synthesized by high temperature polycondensation of 4-fluorophenyl sulfone with 2,5-(4′,4″-dihydroxy biphenyl)-pyridine and tetramethyl biphenyl diol. The chemical structure is depicted

* Corresponding author. Tel.: +30 2610965268; fax: +30 2610965223.
** Co-corresponding author. Tel.: +30 2610965265; fax: +30 2610965223.
E-mail addresses: geoavg@iceht.forth.gr (G. Avgouropoulos), neoph@iceht.forth.gr (S. Neophytides).

0926-3373/$ – see front matter © 2009 Elsevier B.V. All rights reserved.
doi:10.1016/j.apcatb.2009.04.025

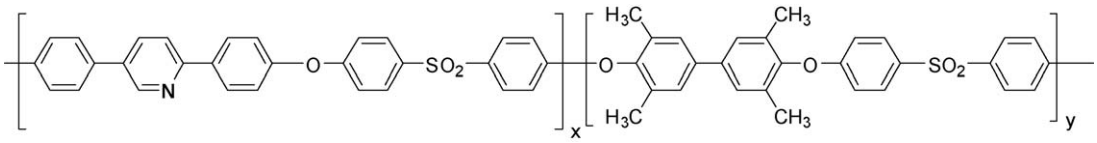

Scheme 1. Chemical structure of copolymer TPS®.

in Scheme 1. Solvents were purchased from Aldrich and used without further purification.

2.1. Casting and doping of copolymer TPS® electrolyte membrane

TPS® copolymer was dissolved in dimethylacetamide (DMAc) at room temperature. The solvent was slowly evaporated at 70 °C (24 h) and dried in vacuum at 160 °C (72 h) resulting into a polymer film of 70 μm thickness. The membrane was immersed in 85 wt.% phosphoric acid at 130 °C (48 h) in order to reach a doping level 180 wt.%.

2.2. Membrane electrode assembly

The catalytic layer was sprayed onto the carbon/teflon gas diffusion layer, which was supported on carbon cloth provided by ETEK [13]. The catalyst ink was a DMAc suspension comprising 1:1 by weight HP E-TEK Pt/C catalyst and TPS® as binder. The electrode loading was 1 mg Pt/cm^2. The electrode was treated in a vacuum oven at 190 °C for solvent removal.

The Pt/C electrodes were hot pressed at 150 °C and 10 bar (25 min) to the TPS® acid-doped polymer electrolyte membrane in a die set up using Teflon (Dupont, USA) and FEP gaskets to achieve the appropriate compression and sealing in the single cell.

2.3. Reforming catalyst

6.5 g of Cu–Mn–O (atomic ratio Cu/(Cu + Mn) = 0.30) spinel oxide supported on Cu foam (M-Pore, 30 ppi, 8 cm^2 × 1 cm thickness) was prepared via the combustion method and used as methanol reforming catalyst, without additional oxidation or reduction pretreatments [14]. The Cu metal foam was immersed for a few seconds in an aqueous solution of urea and nitrate salts of copper and manganese, mixed in the appropriate molar ratios. Then, it was removed and the excess solution was blown out by hot air ejected from a heat gun set at 150 °C. The temperature of the heat gun was subsequently raised to 500 °C and immediately the combustion reaction started with evolution of a large quantity of gases and the gel-coated foam changed color, indicating the formation of Cu–Mn oxide solids on the surface. This procedure was repeated several times in order to achieve the desired catalyst loading.

2.4. Fuel cell measurements

An 8 cm^2 internal reforming methanol single fuel cell was prepared according to the proposed configuration described in Fig. 1. The fuel cell was composed of a membrane electrode assembly described in Section 2.1 comprising a TPS® phosphoric acid-doped copolymer, as the high temperature polymer electrolyte membrane, sandwiched between the anodic (Cu–Mn spinel oxide supported on metallic copper foam for the production of CO-free hydrogen and placed adjacent to the Pt/C anode electrocatalyst) and Pt/C cathodic gas diffusion electrodes. Vaporized methanol and water mixtures (H_2O/CH_3OH = 1.5; He as balance) were supplied to the anode compartment, where the reforming catalyst is directly adjoined with the anode electrode, according to Fig. 1. The total flow rate was 40 cm^3 min^{-1} (STP). Pure oxygen was supplied to the cathode compartment at a flow rate of 50 cm^3 min^{-1} (STP). The cell temperature was set at 200 °C. The cell performance was evaluated at atmospheric pressure under three different feedstreams: (i) Feed 1: 6.5% CH_3OH/9.75% H_2O/He, (ii) Feed 2: 13% CH_3OH/19.5% H_2O/He and (iii) Feed 3: 20% CH_3OH/30% H_2O/He. A mass spectrometer (Omnistar/Pfeiffer Vacuum) was used for online monitoring of effluent gases. Product analysis was also done by a gas chromatograph (Agilent Technologies, 6820 GC

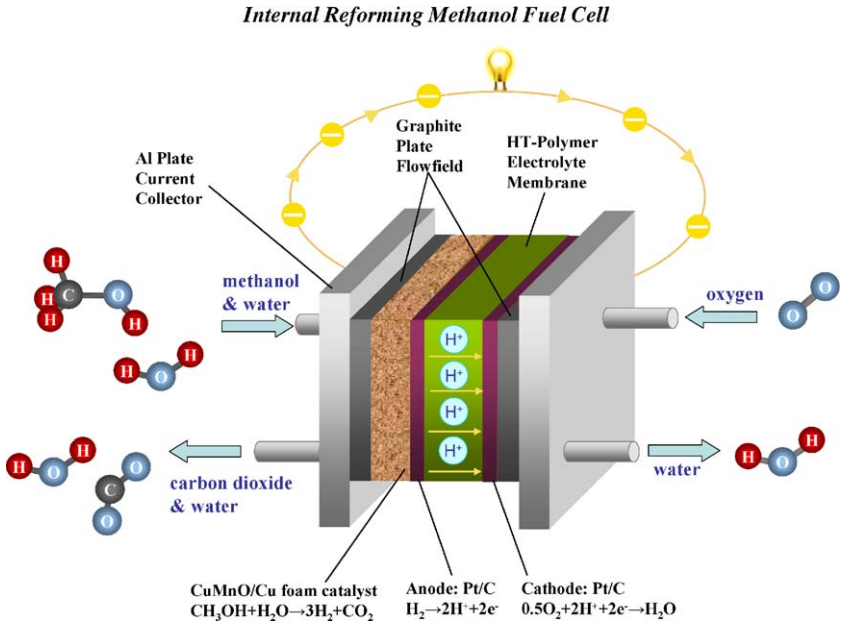

Fig. 1. IRMFC configuration.

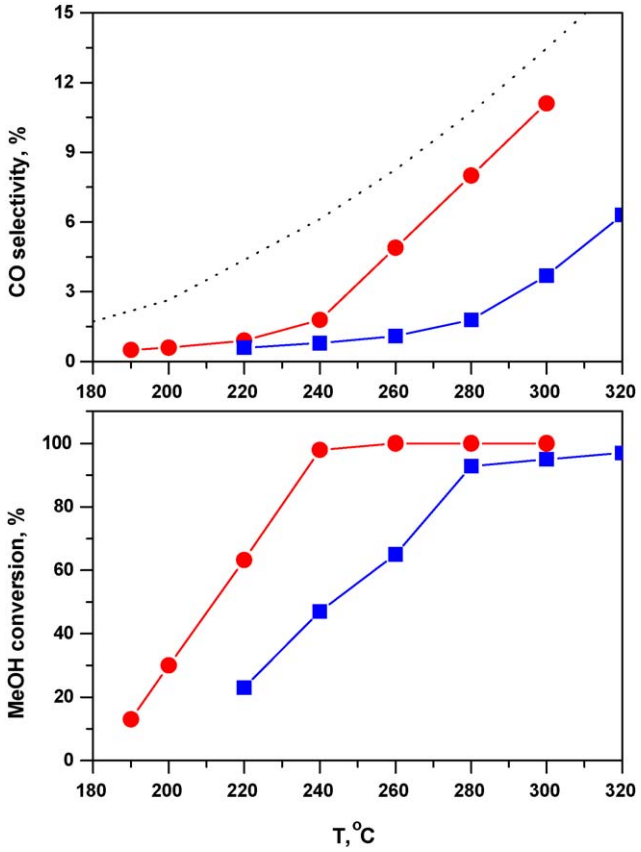

Fig. 2. Activity and selectivity for the steam reforming of methanol over combustion-synthesized Cu–Mn–O/foam catalyst. Operating conditions: $W/F = 0.257$ g s cm^{-3}, 5% CH_3OH (●), 32% CH_3OH (■), $H_2O/CH_3OH = 1.5$. Dotted line represents the CO equilibrium selectivity. Data reproduced from Ref. [14].

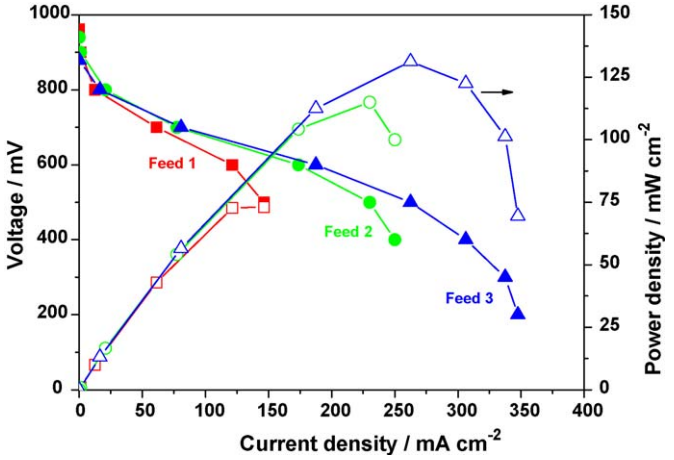

Fig. 3. IRMFC polarization curves under various methanol/water feeds at 200 °C. The following gas mixtures were supplied to the anode via a syringe pump at a total flow rate of 40 cm^3 min^{-1} (STP): Feed 1 (■): 6.5% CH_3OH/9.75% H_2O/He, Feed 2 (●): 13% CH_3OH/19.5% H_2O/He, Feed 3 (▲): 20% CH_3OH/30% H_2O/He. Pure O_2 was supplied to the cathode; $T_{cell} = 200$ °C; $P_{cell} = 1$ atm. Solid symbols: cell voltage vs. current density; open symbols: power density vs. current density.

System) equipped with TCD and FID. The electrochemical measurements were carried out by an AMEL potentiostat/galvanostat model 7060.

3. Results and discussion

In the present study, we combine the low temperature Cu–Mn–O methanol steam reforming catalyst [1], supported on the surface of a monolithic structure [14] (such as metallic copper foam), which also plays the role of current collector, in direct contact to the anode electrode of a high temperature polymer electrolyte membrane electrode assembly (MEA) [15] (Fig. 1). The MEA comprises Pt/C electrodes interfaced with the H_3PO_4-imbibed, high-temperature polymer electrolyte membrane of novel chemical structure, bearing main chain pyridine units [12] as polar groups, which was synthesized so as to satisfy the operating conditions as a high temperature polymer electrolyte in the present application. The aromatic polyether's structure ensures excellent chemical and thermal stability ($T_d > 400$ °C). The pyridine units are protonated by H_3PO_4 following an acid–base type reaction so that the membrane is imbibed with H_3PO_4 at a doping level as high as 180 wt.%. Beyond their high proton conductivity (>0.06 S cm^{-1} at 180 °C) these polymer structures are characterized by high molecular weight (MW = 65,000–80,000 Da), excellent film forming properties and high glass transition temperature (280 °C) which results in very good thermal and mechanical stability being reliable for long term fuel cell operation at 200 °C. In addition one of the most significant properties of these MEAs is their ability to retain H_3PO_4 so that it would not leach to the Cu–Mn–O catalyst due to the high operating temperature.

Cu–Mn–O materials have been proven to be very efficient methanol steam reforming catalysts, able to selectively produce CO_2 and H_2 at temperatures lower than 240 °C, as shown in Fig. 2 [1,14,15]. The structural and morphological properties of Cu–Mn spinel oxide catalysts were investigated and discussed in detail in previous papers by Papavasiliou et al. [1,14]. It was found that the combustion method is an efficient technique for direct formation of Cu–Mn oxide layers on the surface of metallic foams [14]. The foam catalysts had similar structural characteristics with powder catalysts. The adhesion of the catalyst layers on the metal foam was good and the performance of these foam catalysts in the reaction of methanol reforming was in-line to the one of unsupported powder catalysts also prepared with the combustion method. Despite their low surface areas (<9 m^2 g^{-1}), these catalysts had comparable activity to that of a commercial $Cu/ZnO/Al_2O_3$ catalyst for the production of H_2 via (combined) steam reforming of methanol [1,14]. The fresh Cu–Mn catalysts were composed of the spinel phase $Cu_{1.5}Mn_{1.5}O_4$, as well as Mn_2O_3 and CuO, depending on the Cu/Mn ratio, and were reduced to Cu^0 and MnO under reaction conditions. XPS analysis revealed the presence of two different oxidation states in both copper (Cu^{2+} and Cu^+) and manganese (Mn^{4+} and Mn^{3+}) in fresh catalysts and decomposition of the spinel in used catalysts. The optimal catalyst was prepared with a Cu/(Cu + Mn) ratio of 0.30. This ratio was applied in the present study. The amount of CO produced from reforming was well below water–gas shift equilibrium (Fig. 2), in accordance with the present study where only traces of CO were detected at 200 °C. Other by-products such as formaldehyde, formic acid, methyl formate or dimethyl ether, which are often formed by reactions of methanol over Cu-based catalysts, were not detected in the present study at 200 °C. Thus, CO_2 was the only carbon-containing product, whereas traces of CO were produced by the reverse water–gas shift reaction, resulting in almost 100% H_2 selectivity. Previous TPO measurements after methanol reforming runs over Cu–Mn catalysts indicated only minimal carbon deposition [1].

In the present study, the deposition of Cu–Mn oxide catalyst on the porous metallic foam provides fast heat conductivity and uniform temperature distribution for the endothermic steam reforming reaction, uniform flow distribution and good electrical conductivity as current collector (Fig. 1).

Fig. 3 shows typical *I–V* and *I–P* curves for anode feeds with different methanol concentrations. In all three cases shown in Fig. 3, the open circuit cell potential is at the same value to the corresponding cell potential under H_2. This is attributed to H_2 that is being produced by the steam reforming process and readily interacts with the Pt/C anode electrode. The peak power density is 125 mW cm^{-2} at the highest methanol concentration (20% CH_3OH). It is worth noticing that by feeding the cell with similar H_2 molar fraction to the corresponding H_2 content that is being produced by the steam reforming reaction the current–voltage and power characteristics of the cell are very similar to those depicted in Fig. 3. This implies that the anode's performance is not affected by the presence of methanol, water or CO_2. In all three cases depicted in Fig. 3 methanol conversion was above 75%, while the sharp decrease in cell voltage and power output at high current densities is due to H_2 starvation.

It is worth noticing that at current densities up to 200 mA cm^{-2} the performance of the cell is similar to the performance of the solid acid methanol fuel cell operating already at 240 °C as reported in Refs. [8–10]. Certainly the operation of an experimental single cell differs on several engineering aspects with regards to the operation of a fuel cell stack. Thus, the design and the construction of a stack must take into consideration the fact that only vaporized mixture of methanol and water will be fed to the stack. The H_2O/CH_3OH ratio will be determined by the kinetics of SRM reaction, while the endothermicity of the SRM reaction and excess water must be taken into consideration for the design of the cooling system of the fuel cell stack.

The most significant observation of the present study is depicted in the transient experiment of Fig. 4 and refers to the positive effect on the catalytic reforming reaction rate during fuel cell operation. Fig. 4 is divided into three regions:

- The anode feedstream composition (fuel cell bypass) is presented in region (A).
- Region (B) depicts the steady state profiles of methanol catalytic steam reforming reaction for CO_2 and H_2 formation reaction rates and the non-converted flow rates of H_2O and CH_3OH. The reaction takes place over Cu–Mn–O foam catalyst placed in the anode compartment. Since the fuel cell is not in operation (open circuit conditions $I = 0$) the profiles in region (B) represent the net catalytic reaction rate.
- Region (C) represents the reactants and products responses after the fuel cell has been turned on (at $t = t_0$: $I = 1.7$ A at 0.5 V).

As expected upon turning on fuel cell at $t = t_0$ (Fig. 4), a sharp decrease is observed on H_2 concentration, which is apparently attributed to its consumption due to fuel cell operation. Simultaneously it is interestingly shown, that methanol's consumption rate increases by 12.2% (93.4% final methanol conversion). Unexpectedly and within the time frame of the transient experiment, a 33% increase is recorded in the reaction rate of CO_2 production being approximately three times higher than the consumption rate of methanol. This discrepancy in carbon balance can be rationalized only by considering non-steady state conditions during the transient electrochemical extraction of H_2 from the gas phase, so that the various adsorbed intermediates will adjust to the new gas phase composition. It is rather possible that the electrochemical extraction of H_2 affects the oxidation state of the catalytic surface by controlling the coverage of the adsorbed hydroxyl species, thus resulting in the enhancement of the oxidation rate of the various adsorbed carbonaceous intermediates. This is corroborated by the evolution of H_2O consumption rate, which initially shows a sharp decrease in accordance to the sharp increase of CO_2 formation rate, while being also in discordance with the corresponding reaction rate of methanol

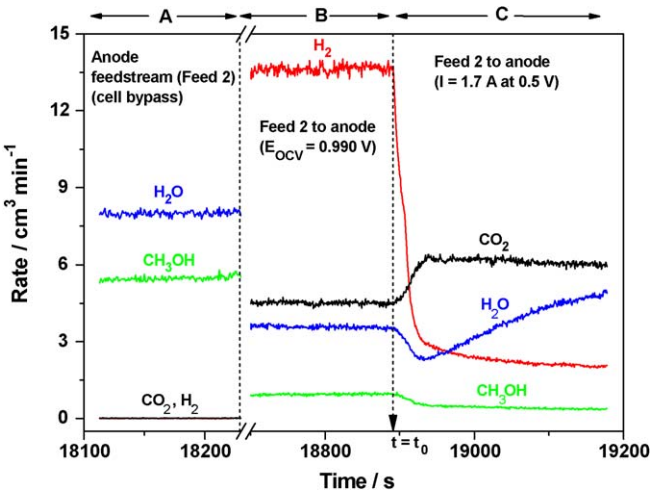

Fig. 4. Transient responses of H_2, H_2O, CO_2 and CH_3OH during current application. At time $t = t_0$ a current $I = 1.7$ A is applied at a cell potential of 500 mV (region C). Anode feedstream (bypass: region A; through anode reforming catalyst and prior current application: region B): Feed 2: 13% CH_3OH/19.5% H_2O/He, 40 cm^3 min^{-1} (STP). Pure O_2 was supplied to the cathode; T_{cell} = 200 °C; P_{cell} = 1 atm.

consumption. Thereafter it is interesting to notice the rather unexpected increase in H_2O content. It originates from the produced H_2O at the cathode that selectively permeates the membrane [16]. H_2O will affect positively the steam reforming reaction due to the positive order kinetics of the reforming reaction with respect to H_2O partial pressure [1].

H_2 can affect either the equilibrium-kinetics of elementary steps that lead to dehydrogenated intermediates from adsorbed methanol or the coverage of OH_{ad} originating from the dissociative adsorption of water. The long transient time interval prior achieving steady state (~20 min, not shown here for brevity) can be rationalized by the high contact time (9.75 g s cm^{-3}) in combination with the large amount of adsorbed intermediates that can be accommodated on the catalyst surface (361 μmol g_{cat}^{-1}) [17]. Very recently, Papavasiliou et al. studied the mechanistic aspects of steam reforming of methanol via steady-state isotopic transient kinetic analysis over copper-based catalysts, including combustion-synthesized Cu–Mn–O catalyst [17]. A parallel reaction mechanism was found to be operative, while the presence of $CH_3{}^{18}OH$ in the products after the switch to ^{18}O-labeled water indicated that the main path of the reaction over the Cu–Mn–O catalyst is the one involving a methyl formate intermediate (Scheme 2). Dehydrogenation and decomposition steps are taking place in the proposed reaction pathway, where the concentration of H_2 plays decisive role by affecting the equilibrium conversions and reactivities of potential adsorbed intermediates such HCHO and $HCOOCH_3$. In these experiments performed at 190 °C, times longer than 20 min were required in order to achieve a new steady state after the isotopic switch. Such long transition times, also evidenced in the present study at 200 °C, are quite usual for methanol, dimethyl ether and methyl formate synthesis as well as methanol steam reforming over Cu-based catalysts [17].

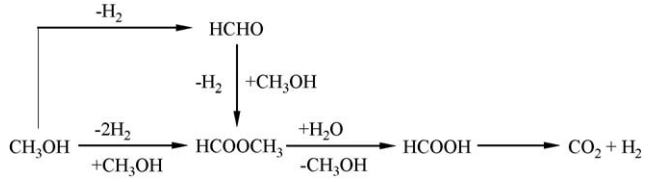

Scheme 2. Predominant reaction pathways for steam reforming of methanol over Cu–Mn–O catalyst on the basis of previous mechanistic studies [17].

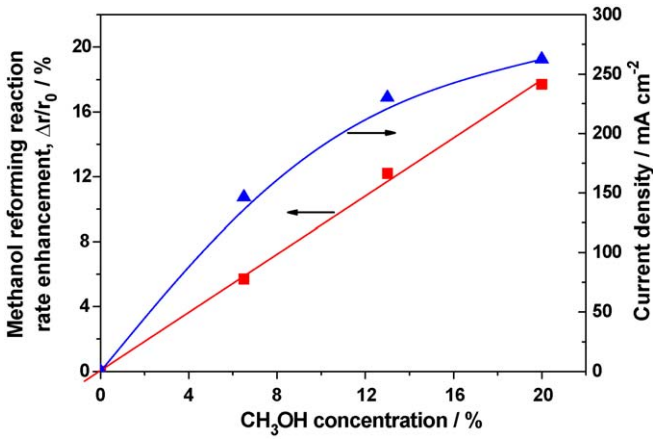

Fig. 5. Methanol reforming reaction rate enhancement and current densities after applying cell voltage of 500 mV at 200 °C. Various methanol/water feeds (H_2O/CH_3OH = 1.5) were supplied to the anode (conditions as in Fig. 2) via syringe pump at a total flow rate of 40 cm^3 min^{-1} (STP). Pure O_2 was supplied to the cathode; T_{cell} = 200 °C; P_{cell} = 1 atm.

In general the transient experiment of Fig. 4 shows the inhibiting role of H_2 on methanol steam reforming reaction kinetics. As depicted in Fig. 5 the steady state rate enhancement increases linearly with increasing methanol concentration (H_2O/CH_3OH = 1.5) and cell current (at 0.5 V). This increase can be attributed to the positive reaction kinetics of the SRM reaction with respect to methanol and water partial pressure. The effect of water and methanol partial pressure on the SRM reaction over Cu–Mn oxide catalysts was examined in a previous work [1], with experiments performed under differential reaction conditions. The overall reaction order of methanol reforming with respect to reactants was 1.2 (0.7 for methanol and 0.5 for water). The reported values in the literature are generally in the range of 0.2–0.6 for methanol and 0.02–0.4 for water, while CO_2 was found to have negligible effect on the overall reaction rate [1]. In many cases, a negative reaction order with respect to hydrogen partial pressure has been reported [1]. Electrochemical pumping of H_2 through the fuel cell membrane itself alleviates the inhibiting effect of H_2, thus inducing a promotional kinetic effect on the catalytic activity. In the present study the obtained final methanol conversions are 99.1, 93.4 and 83.5% corresponding to anode feed streams containing 6.5, 13 and 20% methanol. The rate enhancement at the highest methanol concentration is 17.7%, whereas the linear variation denotes even higher promotional effect at higher methanol concentrations.

A similar effect of H_2 was observed by Samms and Savinell [11] who studied the kinetics of methanol steam reforming over Cu/ZnO/Al_2O_3. The enhancement of the steam reforming reaction rate has been also observed in membrane reactors, where H_2 is selectively removed from the main reaction stream [18]. However, the rate enhancement was erroneously attributed to the positive shift of the equilibrium conversion of the steam reforming reaction rate, while it is well known that methanol steam reforming reaction is not confined by equilibrium constrains due to the negative free Gibb's energy of the reaction at temperatures around 200 °C (ΔG = −41.7 kJ mol^{-1}) [19]. Nevertheless the inhibiting role of H_2 on the kinetics of the steam reforming reaction can be rather attributed to the effect of H_2 content on reactions of surface intermediates, such as methoxy, adsorbed formaldehyde and formate species. In addition the variation of the partial pressure of H_2 is expected to affect the equilibrium of the dissociative adsorption of water, thus resulting in the increase of hydroxyl species coverage. In this respect the kinetics of the oxidation reactions can be promoted too. The promoting effect of H_2 depletion will result to a corresponding decrease of catalyst loading and the simplification of the overall balance of the system in terms of its structural architecture.

4. Conclusions

In summary it has been shown that it is technically feasible to combine the concepts of methanol reformer and PEM fuel cell in a single and compact arrangement. The proposed internal reforming methanol high temperature PEM fuel cell (IRMFC) mainly comprises: (i) a H_3PO_4-imbibed polymer electrolyte based on aromatic polyethers bearing pyridine units, able to operate at 200 °C and (ii) a Cu–Mn–O methanol reforming catalyst supported on copper foam active at 200 °C with zero CO emissions. The latter is incorporated into the anodic compartment of the fuel cell, so that methanol reforming takes place inside the cell (internal reforming). The "waste" heat of the cell is utilized *in situ* to drive the endothermic methanol reforming reaction. The IRMFC operated efficiently for more than 72 h at 200 °C with a current density of 263 mA cm^{-2} at 500 mV, when 20% CH_3OH/30% H_2O/He (anode feed) and pure O_2 (cathode feed) were supplied. Its open circuit voltage was 990 mV. Due to H_2 utilization/depletion at the anode the reforming reaction rate was enhanced even up to 20%.

Acknowledgement

This research was carried out under APOLLON-B project financed by the EC within the FP6-2004-NMP-TI-4.

References

[1] J. Papavasiliou, G. Avgouropoulos, T. Ioannides, J. Catal. 251 (2007) 7–20.
[2] N. Liu, Z. Yuan, C. Wang, L. Pan, S. Wang, S. Li, D. Li, S. Wang, Chem. Eng. J. 139 (2008) 56–62.
[3] C. Song, Catal. Today 77 (2002) 17–49.
[4] A. Biyikoglu, Int. J. Hydrogen Energy 30 (2005) 1181–1212.
[5] S. Patel, K.K. Pant, Chem. Eng. Sci. 62 (2007) 5425–5435.
[6] H. Liu, C. Song, L. Zhang, J. Zhang, H. Wang, D.P. Wilkinson, J. Power Sources 155 (2006) 95–110.
[7] C. Pan, R. He, Q. Li, J.O. Jensen, N.J. Bjerrum, H.A. Hjulmand, A.B. Jensen, J. Power Sources 145 (2005) 392–398.
[8] S.M. Haile, T. Uda, US Patent 2005/0271915 December 8 (2005).
[9] D. Boysen, T. Uda, C.R.I. Chisholm, S.M. Haile, Science 303 (2004) 68–70.
[10] T. Uda, D. Boysen, C.R.I. Chisholm, S.M. Haile, Electrochem. Solid-State Lett. 9 (2006) 261–264.
[11] S.R. Samms, R.F. Savinell, J. Power Sources 112 (2002) 13–29.
[12] E.K. Pefkianakis, V. Deimede, M.K. Daletou, N. Gourdoupi, J.K. Kallitsis, Macromol. Rapid Commun. 26 (2005) 1724–1728.
[13] N. Gourdoupi, N. Triantafyllopoulos, V. Deimede, L. Pefkianakis, M. Daletou, S. Neophytides, J. Kallitsis, US Patent 20080063923, March 13 (2008).
[14] J. Papavasiliou, G. Avgouropoulos, T. Ioannides, Appl. Catal. B: Environ. 66 (2006) 168–174.
[15] G. Avgouropoulos, J. Papavasiliou, M. Daletou, M. Georgezi, N. Triantafyllopoulos, T. Ioannides, J. Kallitsis, S. Neophytides, US Patent 200861/095779, September 10 (2008).
[16] M.K. Daletou, J.K. Kallitsis, G. Voyiatzis, S.G. Neophytides, J. Membr. Sci. 326 (2009) 76–83.
[17] J. Papavasiliou, G. Avgouropoulos, T. Ioannides, Appl. Catal. B: Environ 88 (2009) 490–496.
[18] A. Iulianelli, T. Longo, A. Basile, J. Membr. Sci. 323 (2008) 235–240.
[19] R.C. Reid, J.M. Prausnitz, B.E. Polling, The Properties of Gases & Liquids, 3rd ed., McGraw-Hill, 1987.